ACS APPLIED MATERIALS & INTERFACES

Research Article

www.acsami.org

Highly Sensitive Colorimetric Cancer Cell Detection Based on Dual Signal Amplification

Tao Yu, Pan-Pan Dai, Jing-Juan Xu,* and Hong-Yuan Chen*

State Key Laboratory of Analytical Chemistry for Life Science and Collaborative Innovation Center of Chemistry for Life Sciences, School of Chemistry and Chemical Engineering, Nanjing University, Nanjing 210023, China

Supporting Information

ABSTRACT: Facile and efficient detection of cancer cells at their preclinical stages is one of the central challenges in cancer diagnostics. A direct, rapid, highly sensitive and specific biosensor for detection of cancer biomarkers is desirable in early diagnosis and prognosis of cancer. In this work, we developed, for the first time, an easy and intuitive dispersion-dominated colorimetric strategy for cancer cell detection based on combining multi-DNA released from an aptamer scaffold with cyclic enzymatic amplification, which was triggered by aptamer DNA conformational switch and demonstrated by non-cross-linking gold nanoparticles (Au NPs) aggregation. First, five kinds of messenger DNAs (mDNAs) were aligned on the cancer cell aptamers modified on magnetic beads (MBs) to form mDNAs-Apt-MBs biocompatible nanosensors. In the presence of target cells, the aptamer would bind to the receptors on the cell membranes, and mDNAs would be released, resulting in the first amplification that one biological binding event would cause the release of multiple kinds of mDNAs simultaneously. After magnetic separation, the released mDNAs were introduced into the cyclic enzymatic amplification to cleave more single strand DNA (ssDNA) fragments. Instead of modification of Au NPs, these fragments and mDNAs could be adsorbed on the surface of Au NPs to prevent particle aggregation and ensure the stability and color of solution in high salt environments. The linear response for HL-60 cells in a concentration range from 10 to 10^4 cells was obtained with a detection limit of four cells in buffer solution. Moreover, the feasibility of the proposed strategy was demonstrated in a diluted serum sample. This dual signal amplification method can be extended to other types of cancer cells, which has potential application in point-of-care cancer diagnosis.

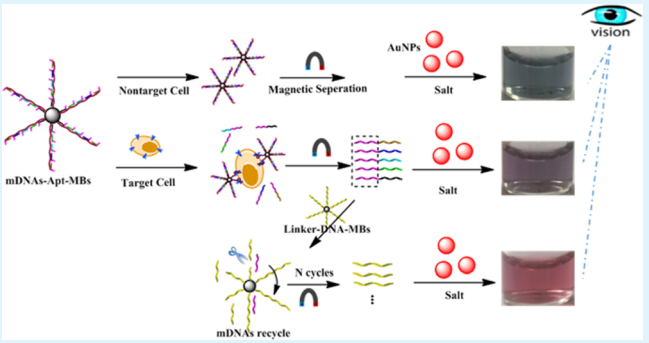

KEYWORDS: *colorimetric detection, cancer cells recognition, aptamer, magnetic nanoparticle, gold nanoparticles, dual signal amplification*

INTRODUCTION

Strategies that enable early detection of cancer cells with high selectivity and sensitivity are highly desired in cancer diagnostics and therapy.[1−3] Different from normal cell lines, a certain cancer cell line has its specific intracellular or extracellular biomarkers, as indicators of the state of disease.[4] Compared with diagnosing suspected cancer, looking for strategies that can detect cancer cell through specific molecular recognition of its biomarkers greatly improve early diagnosis and prognosis of cancer.[4,5] Aptamers, as a novel class of ligands, are single stranded RNA or DNA oligonucleotides which have distinct recognizing properties to various targets, including proteins, small molecules, and even entire cells.[5−7] In recent years, many new cancer cell aptasensors with various signal readout techniques have been developed, such as colorimetric detection,[8−11] fluorescence,[12−14] chemiluminescence,[15] electrochemical,[16,17] and magnetic field.[18,19] Wherein, colorimetric analysis has attracted special concern due to merits of simple, low cost, quick feedback, and no need of any complicated instrumentation.[20,21]

To transform the aptamer-target binding events into color signals, a number of sensitive noninstrument colorimetric detection approaches have been developed based on combining biomolecular recognition events with a series of nanomaterials.[22−24] Among all existing and emerging materials, gold nanoparticles (Au NPs) have been confirmed to be an excellent candidate for bioassays due to their straightforward preparation/modification protocols and red-to-purple (or blue) color change based on the surface-plasmon resonance (SPR) properties, which can be conveniently readout by naked eyes or detected by plasmonic absorbance.[25,26] The target-induced aggregation of Au NPs has been widely used to detect specific analytes such as protein, metal ions, and cells in the past years.[27−29] One of the obstacles against large-scale practical application in early cancer diagnosis, however, is that the color change of Au NPs is not particularly evident due to a relatively

Received: December 11, 2015
Accepted: January 29, 2016
Published: January 29, 2016

DOI: 10.1021/acsami.5b12117
ACS Appl. Mater. Interfaces 2016, 8, 4434−4441

low quantity of biomarkers on the cancer cell membrane.[30] Therefore, amplifying the detection signal is of great significant in colorimetric detection.

To improve the sensitivity of visual detection, many amplification methods combined with recognition molecules have been developed. Recently, a kind of bimetallic copper−gold nanoparticle (Cu−Au NP) with special response to iodide as an amplified signal probe was introduced to versatile colorimetric analysis method for ultrasensitive detection of targeted cancer cells.[31] Using Au NPs as nano sticky balls to amplify the magnetophoretic effect, an enzyme-free amplification that provided a sensitive visual detection of ssDNA/RNA oligonucleotides was also reported, with a limit of detection of 10 amol for ssDNAs.[32] However, using the color change of tetramethyl benzidine (TMB) usually suffers from the disadvantage of short storage life and the potential toxicity. Besides, a high temperature is needed for using Au NPs as nano sticky balls for enzyme-free amplification, which make the aptasensor unstable and not suitable for point-of-care diagnoses. Until now, only a few amplified strategies are reported for Au NPs-based colorimetric methods in the isothermal conditions.[33,34] Nicking enzyme signal amplification based on endonuclease was confirmed to be an effective means for improving sensitivity, which had been widely used in visual or other types of detection.[35] More importantly, these specific nicking enzyme reactions can be performed in isothermal conditions and no need of specialized instrumentation, which can be widely used in routine analysis.[36] Thus, it is possible that the detection sensitivity of cancer cells could also be improved by combining with the nicking enzyme amplification and aptamer scaffold conformational switch.

In this work, a kind of aptamer-magnetic bead bioconjugate (mDNAs-Apt-MBs), fabricated by five kinds of messenger DNAs (mDNAs) aligned on the cancer cell aptamers modified on MBs, was first synthesized. Having strong special binding ability to cancer cells, mDNAs-Apt-MBs were used as the effective bridge to quantitatively connect cells with recognition molecules, thus contributing to a novel and versatile colorimetric analysis platform. The introduction of HL-60 cells would trigger the conformational switch of the aptamer to release mDNAs, resulting in an amplification method that one biological binding event would cause the release of multiple kinds of mDNAs simultaneously. Then, introducing released mDNAs into the cyclic enzymatic amplification would produce more ssDNA fragments. Finally, based on the above two amplification method, a novel, simple, highly selective and ultrasensitive colorimetric method for cancer cell detection was developed through a further combination with ssDNA inducing antiaggregation ability of Au NPs in high salt solutions, due to the enhanced interparticle repulsion of Au NPs resulted from the additional negative charges of nucleic acids.[37−40] To our best knowledge, our method is the first example that combined the use of non-cross-linking Au NPs aggregation and dual signal amplification to fabricate a sensitive colorimetric cancer cell sensor, which allows us to detect the target cells simply and rapidly and exhibits a significant specificity for HL-60 cells.

EXPERIMENTAL SECTION

Materials and Apparatus. All of the oligonucleotides used in this work were synthesized by Sangon Biotech. Co., Ltd. (Shanghai, China), which were purified by HPLC (Table S1). Fetal bovine serum (FBS), new bovine calf serum (NBCS), Dulbecco's modified eagle medium (DMEM), and penicillin/streptomycin were purchased from Gibco (USA). DNase I endonuclease was purchased from KeyGen Biotech. NEase (Nb.BbvCI) and 10× NEB buffer (500 mM NaCl, 100 mM Tris-HCl, 100 mM $MgCl_2$, and 10 mM dithiothreitol, pH 7.9) were purchased from the New England Biolabs, Inc. Chloroauric acid ($HAuCl_4$), trisodium citrate, N-(3-(dimethylamino)propyl)-N′-ethyl-carbodiimide hydrochloride (EDC), and *N*-hydroxysuccinimide (NHS) were purchased from Aldrich. Next, 0.1 M phosphate buffer solution (PBS; 100 mM PB, 0.2 M NaCl) at pH 8.0 was used for color detection, and Tris buffer solution (25 mM Tris-HCl, 0.15 M NaCl) at pH 8.2 was used for preparation of DNA solutions. All other reagents and chemicals were of at least analytical reagent grade.

Transmission electron microscopy (TEM) was performed with a JEOL model 2000 instrument. The UV−vis absorption spectra were recorded on a Shimadzu UV-3600 UV−vis−NIR photospectrometer (Shimadzu Co., Japan) at room temperature. Dynamic light scattering (DLS) and zeta potential analysis of Au NPs were performed on a Zeta Sizer Nano ZS (Brookhaven Instruments Ltd.). The water used in this paper was purified by a Mili-Q machine (Millipore, U.S.A.).

Preparation of Au NPs. Water-soluble Au NPs were prepared via citrate reduction of $HAuCl_4$ according to the previously described protocol.[40] In brief, 100 mL of aqueous solution of $HAuCl_4$ (1 mM) was heated to reflux under stirring, then 10 mL of trisodium citrate (38.8 mM) was added quickly, resulting in a change in solution color from pale yellow to deep red. The solution was heated under reflux for 20 min and then allowed to cool to room temperature. The prepared colloid Au NPs were stored in brown glass bottles at 4 °C, the average diameter of the prepared gold nanoparticles was about 13 nm as characterized by transmission electron microscope, and their concentration was estimated by UV−vis spectroscopy.

Preparation of Aptamer Modified Magnetic Beads. The mDNAs-Apt-MBs conjugates were fabricated according to the literature by amino-group-modified aptamers attaching onto carboxyl modified MBs, and then hybridized with the messenger DNA sequences.[41] Briefly, 50 μL of carboxyl-modified magnetic bead suspension (5 mg/mL) was activated by 1.0 mL of imidazol-HCl buffer (pH 7.0, 0.1M) containing 20 mg of EDC and 10 mg of NHS for 60 min, and 150 μL of amino-group-modified DNA sequence (10^{-7} M) was activated by 200 μL of imidazole-HCl solution (pH 7.0, 0.1 M) for 30 min. The aptamer and magnetic beads solution were then mixed and continuously reacted for 12 h to form the mDNAs-Apt-MBs, which were magnetically separated and washed thrice by 200 μL of Tris-HCl buffer (0.1 M) and redispersed in 500 μL of Tris-HCl buffer to form a suspension of 0.5 mg/mL mDNAs-Apt-MBs. A total of 200 μL of mDNAs-Apt-MBs suspension was mixed with 200 μL of solution containing five mDNA sequences (10^{-6} M for each). After 2 h of hybridization, the mDNAs-Apt-MBs hybridization complex was magnetically separated and washed thrice with Tris-HCl buffer and then redispersed in 500 μL of Tris-HCl buffer to form a suspension of 0.2 mg/mL magnetic beads for further use.

Linker-DNA-MBs were fabricated with a similar process as described above. Briefly, 50 μL of carboxyl-modified magnetic bead suspension (5 mg/mL) was activated, and then reacted with 150 μL of amino-group-modified DNA sequence (10^{-7} M) for 12 h to form the Linker-DNA-MBs. After being magnetically separated and washed thrice, the Linker-DNA-MBs were redispersed in Tris-HCl buffer to form a suspension of 0.5 mg/mL Linker-DNA-MBs.

Cell Culture. To investigate the selectivity of the biosensor for the detection of different cells, four kinds of cancer cells (HeLa, PC12, MCF-7, and HL-60 cells) were cultured in a humidified atmosphere (37 °C, 95% air and 5% CO_2). HL-60 and PC-12 cells were cultured in DMEM supplemented with 10% new born calf serum (NBCS) and 100 IU/mL penicillin−streptomycin. HeLa cells were cultured in DMEM supplemented with 10% FBS and 100 IU/mL penicillin−streptomycin. MCF-7 cells were cultured in RPMI 1640 supplemented with FBS and penicillin/streptomycin. Cell density was determined using a hemocytometer prior to each experiment.

Cancer Cell Detection. After HL-60 cells were centrifugated and washed with PBS, 100 μL suspension of mDNAs-Apt-MBs conjugates (0.2 mg/mL) was added to a HL-60 cells suspension with certain concentration and incubated under 37 °C for 1 h to release messenger

DOI: 10.1021/acsami.5b12117
ACS Appl. Mater. Interfaces 2016, 8, 4434−4441

Scheme 1. Schematic Representation of the Visual Detection of HL-60 Cells based on Aptamer DNA Conformational Switch and Non-crosslinking AuNPs Aggregation: (A) Blank, (B) Conformational Switch of mDNAs-Apt-MBs, (C) Cyclic Enzymatic Amplification

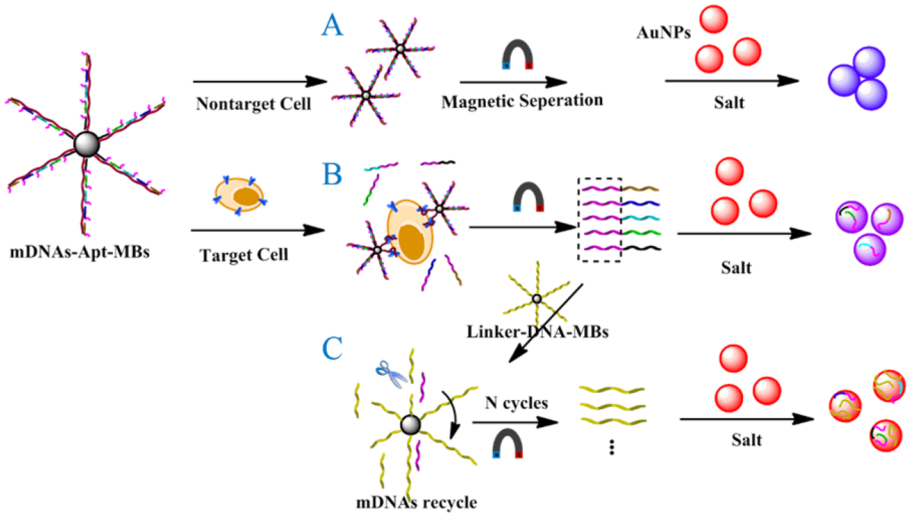

DNA. After magnetic separation, the supernatant was added to the solution containing linker-DNA-MBs, NEase, and NEB buffer at 37 °C for 90 min for nicking endonuclease-strand scission cycles. After magnetic separation again, the suspension was added into 140 μL of Au NPs solution. After incubation for 5 min at room temperature, 160 μL of PBS (pH 8.0, 0.2 M NaCl) was introduced into the mixed solution. The resulting samples were photographed by the mobile phone and tested with a UV−vis spectrometer.

For the cell detection in serum, FBS was diluted with PBS buffer at a ratio of 1:24 before being spiked with HL-60 cells at a different concentration and then performed with the method proposed.

RESULTS AND DISCUSSION

The Mechanism of Colorimetric Assay and Its Dual Signal Amplification. Scheme 1 shows the mechanism of this colorimetric assay for cancer cell detection, which consists of dual signal amplification process by conformational switch of mDNAs-Apt-MBs (Scheme 1B) and cyclic enzymatic amplification (Scheme 1C) and color change process based on the aggregation/dispersion state of Au NPs colloid. Other than traditional methods based on target-induced aggregation of Au NPs, we employ a target-induced dispersion strategy for target cell detection. When the mDNAs-Apt-MBs was incubated with target cells, two-round amplifications were implemented to enhance the sensitivity of this colorimetric assay. First, the introduction of HL-60 cells would trigger the conformational switch of mDNAs-Apt-MBs to release mDNAs. Because of the high volume ratio of cancer cells to magnetic beads and mDNAs-Apt-MBs fabricated by five kinds of mDNAs aligned on the cancer cell aptamers modified on MBs, one cell could make large amounts of mDNAs released simultaneously to amplify the signal. The released mDNAs could be adsorbed on the Au NPs to protect them from aggregation to a certain extent (Scheme 1B). Moreover, it is important to note that these five kinds of mDNAs are single stranded oligonucleotides, each of which consists of two fragments: a short DNA sequence complementary to part of the aptamer probe and a same sequence ATCCTCAGCAGT that can be complementary to part of linker-DNA and recognized by NEase. NEase is a special family of restriction endonucleases, which can recognize a specific sequence known as a restriction site of a double-strand DNA and cleave one strand of it.[42] Second, after magnetic separation, the cyclic enzymatic amplification is implemented by introducing the released mDNAs into the solution containing linker-DNA-MBs, NEase, and NEB buffer. After the mDNAs bonding to linker DNA to form double-stranded structures, the nicking enzyme would bond to and cleave only the linker DNA, resulting in the release of the cleaved linker DNA and free mDNAs from the unstable duplex. The released mDNAs could be reused to hybridize with another linker DNA to form a new duplex for NEase. Finally, each mDNA could go through many scission cycles, leading to cleavage of many ssDNAs (Scheme 1C). Finally, after nicking endonuclease-strand scission cycles and magnetic separation again, the supernatant containing large amounts of ssDNAs fragments was added into Au NPs solution. These ssDNAs were adsorbed on the Au NPs along with mDNAs to prevent particle aggregation and retain the red color of Au NP colloid in high salt environments. With the increased number of target cells, the released mDNAs and cleaved ssDNAs increased correspondingly, and the more dispersive (rather than aggregated) Au NPs were present. In contrast, when target HL-60 cells were absent, the mDNAs-Apt-MBs was intact in solution and no cleaved ssDNA was left after NEase treatment in the following experiment; the introduction of salt will aggregate Au NPs, giving rise to a blue color (Scheme 1A). To further confirm whether this cascade amplifying colorimetric reaction can alter the optical properties of Au NPs, visual photography, UV−vis absorption spectra, and TEM were carried out to test the viability of the colorimetric design.

SsDNA Protecting Au NPs from Aggregation in High Salt Solution. As we mentioned above, single-stranded nucleic acids, having strong attractive electrostatic interactions with citrate coated Au NPs, can make the colloid of Au NPs stabilized in high salt solutions, due to the enhanced interparticle repulsion of Au NPs. To prove this, we used different concentrations of ssDNA to incubate with Au NPs. Figure 1 showed the color change (A) and UV−vis absorption spectra (B) of the Au NPs against different concentration of single strand DNA (23 mers) in 0.1 M PBS containing 0.1 M NaCl. The color of the Au NPs colloid gradually changed from blue to red with the increase of ssDNA concentration, implying an increase in the dispersion state of Au NPs (Figure 1a−g).

DOI: 10.1021/acsami.5b12117
ACS Appl. Mater. Interfaces 2016, 8, 4434−4441

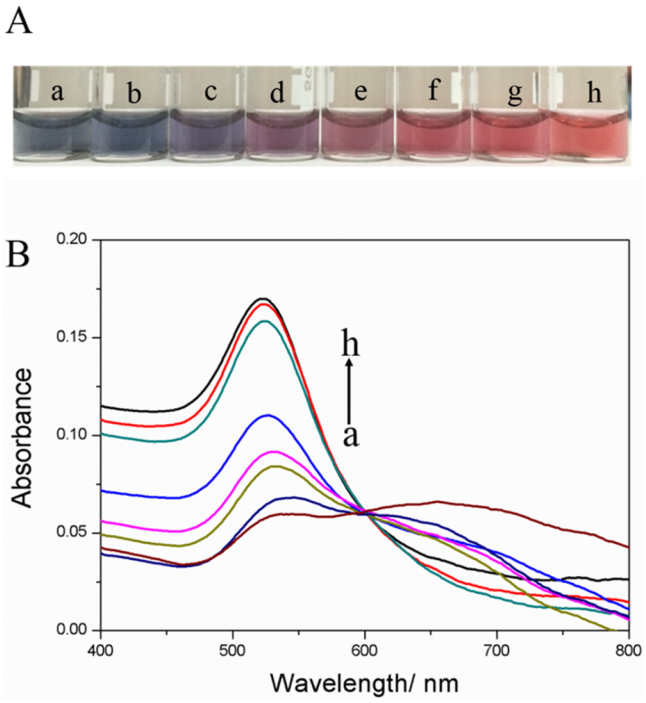

Figure 1. Visual detection (A) and UV−vis absorption spectra (B) of the AuNPs against different concentrations of ssDNA (20 μL for 23 mers). (a−g) 0, 200 nM, 500 nM, 1 μM, 2 μM, 5 μM, 10 μM in 0.1 M NaCl solutions and (h) pure AuNPs solution as standard.

Because the absorbance ratio is related to the color of the Au NPs solution in this study, we used the ratio of absorbance intensities at 525 and 680 nm (A_{525}/A_{680}) to assess the degree of the Au NPs dispersion/aggregation, with a high ratio corresponding to a red solution (dispersion) and a low ratio corresponding to a blue one (aggregation). We find that 0.1 M NaCl no longer causes aggregation of the Au NPs, and the colloid retains a red color (Figure 1f) if enough single stranded oligonucleotide is added to the gold colloid before the addition of the salt that would otherwise cause aggregation. Thus, in this work, the colorimetric assay for cancer cell detection is based on the color change of non-cross-linking Au NPs described above.

Feasibility of the Method for the Detection of HL-60 Cells. To demonstrate the utility of our design, we employed HL-60 cells as model target cells. In the presence of HL-60 cells (1×10^4 cells/mL), after a two-round signal amplification process by conformational switch of mDNAs-Apt-MBs and cyclic enzymatic amplification, the red Au NPs solution retained its original color and a narrow UV−vis absorption peak appeared at 525 nm (Figure 2A,a), implying that the Au NP still retained its dispersed state because of enough ssDNA fragments cleaved from the linker-DNA. The TEM image was also used to verify that the ssDNA would help maintain the dispersion state of Au NPs (Figure 2B). While with only conformational switch of the mDNAs-Apt-MBs process (Scheme 1B), a purple Au NP colloid was observed (Figure 2A,b), with the moderate aggregation of Au NPs as shown in Figure 2C. This was because only released mDNAs were adsorbed on Au NPs with no ssDNAs fragments resulted from the cleavage of linker-DNA on MBs. In addition, blue solution was observed and an UV−vis absorption peak increased clearly at 680 nm in the absence of HL-60 cells (Scheme 1A, Figure 2A,c), showing that the Au NPs in high salt solutions become the aggregation state without any protection from mDNAs or ssDNA fragments, which also could be confirmed by TEM results (Figure 2D). When curve a was compared with b and c, it was clear that NEase could work in this system and effectively cleave the linker DNA after being hybridized with mDNAs in the presence of target cells. In addition, the UV−vis spectroscopy served as complementary evidence along with TEM results to clearly support our method for the detection of cancer cells based on the colorimetric aptasensor.

Optimization of Experimental Conditions. In order to achieve the best performance for detecting cancer cells, the experimental conditions, including the number of mDNAs aligned on a single aptamer, NEase concentrations, and NEase nicking time played important roles in the detection of cancer cells and signal amplification and were investigated.

The key point of our strategy was based on the mDNAs released from the MBs surface in the presence of HL-60 cells. Usually, one aptamer recognizes specific protein to release or

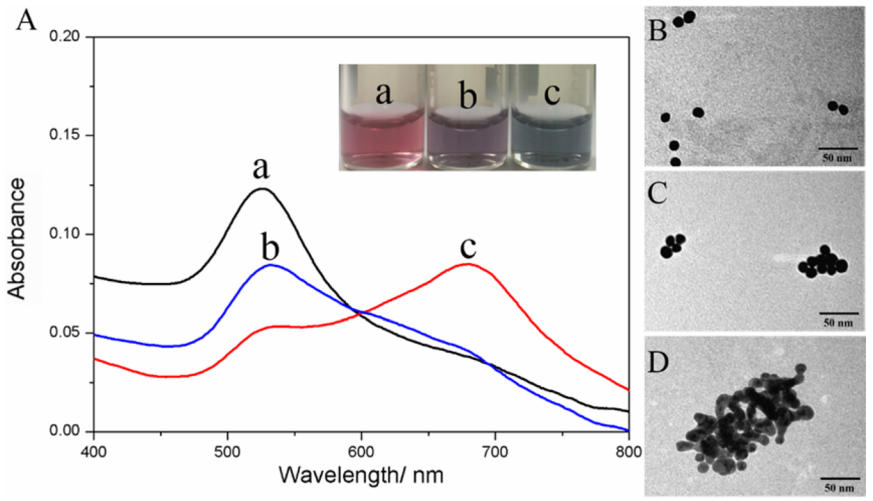

Figure 2. Feasibility of the colorimetric method for detecting HL-60 cells. (A) Absorption spectra and photograph (inset) of AuNPs under different conditions. The system contained mDNAs-Apt-MBs, linker-DNA-MBs, HL-60 cells (1×10^4 cells), and NEase (20 U) (a) but without cyclic enzymatic amplification (b) or HL-60 cells (c). (B, C, D) TEM images of the three statuses of AuNPs.

DOI: 10.1021/acsami.5b12117
ACS Appl. Mater. Interfaces 2016, 8, 4434−4441

reveal a single mDNA.[33,34,44,45] However, in this method, five mDNAs all partly hybridized with one aptamer sequence were used to amplify the signal (Figure 3A). The mDNAs-Apt-MBs

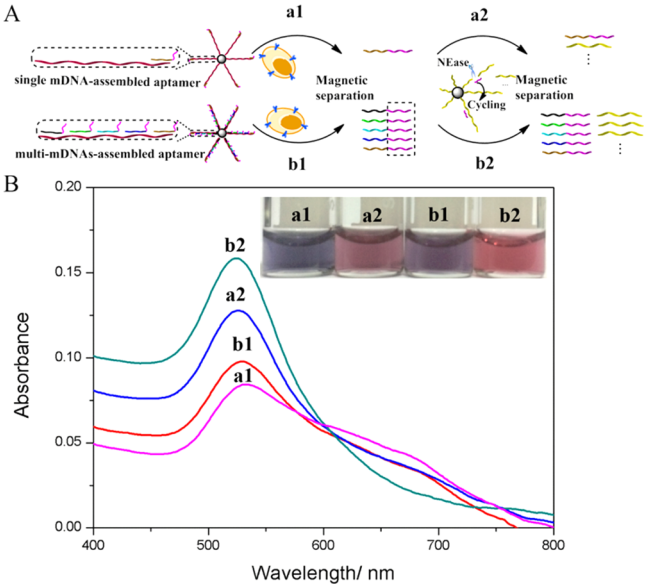

Figure 3. (A) Schematic representation of different quantities of mDNA assembled in single aptamer strand: (a) mDNA1; (b) five mDNAs, mDNA1, mDNA2, mDNA3, mDNA4, and mDNA5, affect the assay before (a1, b1) and after cyclic enzymatic amplification (a2, b2). (B) Absorption spectra and photograph (inset) of Au NPs for detection of HL-60 cells (1×10^4 cells) with different quantities of mDNA in a single aptamer strand.

bind to target cells through the specific interaction between receptors on the cell membranes and aptamers, resulting in one biological binding event releasing multiple kinds of mDNAs simultaneously. These mDNAs, containing the same 12 bases TCCTCAGCAGT, would then be introduced into the cyclic enzymatic amplification process. Therefore, a highly sensitive colorimetric strategy for detection of HL-60 cells based on dual signal amplification could be obtained. In order to prove this point, the UV−vis absorption spectra and pictures (inset) of Au NPs after detection of HL-60 cells (1×10^4 cells/mL) by this colorimetric method with one (a) and five (b) mDNAs in a single aptamer strand were obtained, as shown in Figure 3B. As for first round amplification, the color of Au NPs with using five kinds of mDNA-assembled mDNAs-Apt-MBs (b1 process) was partial to purple, while that of using one kind of mDNA-assembled mDNAs-Apt-MBs (a1 process) was blue, and a higher absorption peak at 525 nm for dispersed Au NPs was observed for five kinds of mDNA-assembled mDNAs-Apt-MBs. All of this suggested that more mDNAs from five kinds of mDNA-assembled aptamer-MBs were released to protect Au NPs from aggregation by the conformational switch process. As for second round amplification, the photograph of Au NPs with using five kinds of mDNA-assembled mDNAs-Apt-MBs (b2 process) was a red color, while that of using one kind of mDNA-assembled mDNAs-Apt-MBs (a2 process) was purple. The UV−vis absorption peak located at 525 nm were both elevated compared with the first round, and the absorption peak after the b2 process is much higher than that of a2, indicating that more ssDNA was cleaved. When process b was compared with a, with equal target cells, it was clear that using multiple kinds of mDNA hybridization systems would result in more mDNAs being released from a conformational switch of mDNAs-Apt-MBs and then more ssDNAs being cleaved from the cyclic enzymatic reaction, which was beneficial for protecting the Au NPs from aggregation and thus improving the detection signal. So multiple kinds of mDNAs were chosen to assemble the mDNAs-Apt-MBs in the dual signal amplification assay.

Different concentrations of NEase (0−50U) incubated with linker-DNA-MBs and message DNA fragments were investigated. As seen in Figure 4A, the A_{525}/A_{680} ratio increased with

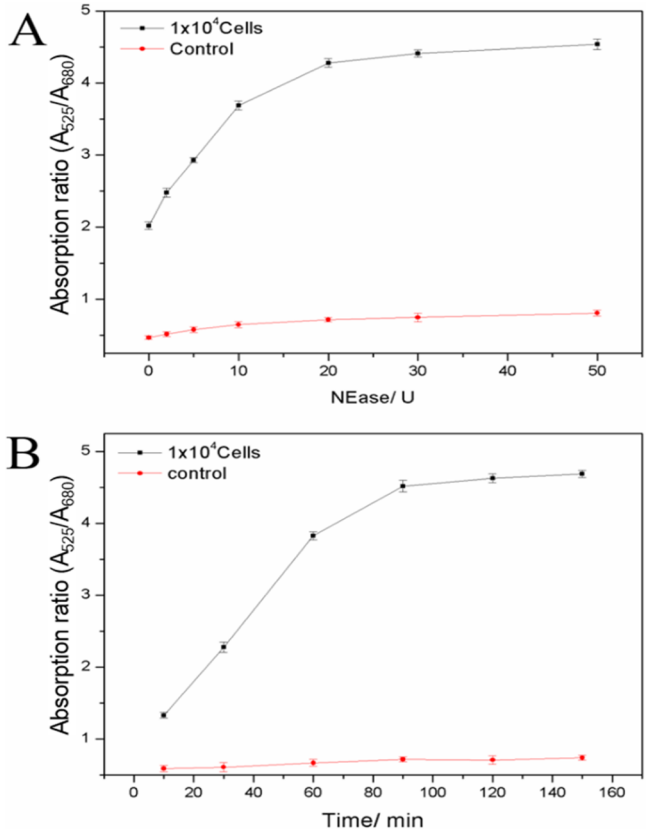

Figure 4. (A) The absorption ratio plotted as a function of the NEase concentration in the absence (red line) or in the presence (black line) of HL-60 cells, respectively. The system contained mDNAs-Apt-MBs (0.2 mg/mL), linker-DNA-MBs (0.2 mg/mL), and HL-60 cell (1×10^4 cells). (B) The absorption ratio was plotted as a function of the nicking time in the absence (black line) or in the presence (red line) of HL-60 cells, respectively. The system contained mDNAs-Apt-MBs (0.2 mg/mL), linker-DNA-MBs (0.2 mg/mL), NEase (20 U), and HL-60 cell (1×10^4 cells). Error bars represent the standard deviation of three measurements.

the increase of NEase concentration in the initial stage and attained a relatively stable plateau at 20U Nease (black line). Meanwhile, with no target cells, the background signal changed little while changing the concentration of Nease (red line), which indicated that the increased NEase concentration was beneficial for the cleavage of linker DNA, and 20 U NEase could attain a better signal-to-noise ratio for the analysis of rare cancer cells. Kinetic studies of nicking time were also performed to study the nicking process by measuring the A_{525}/A_{680} ratio under the same conditions (Figure 4B). We recorded the ratio under conditions with or without target cells. In the presence of target cells, the signal ratio elevated quickly during the initial stage and increased slowly after 90 min (black

DOI: 10.1021/acsami.5b12117
ACS Appl. Mater. Interfaces 2016, 8, 4434−4441

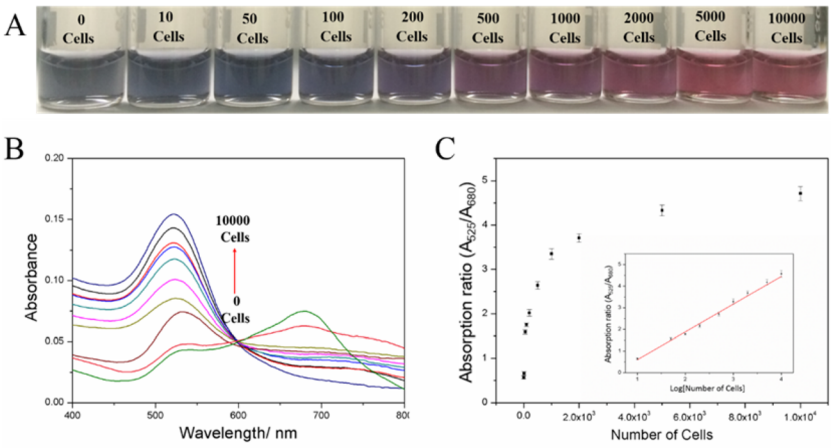

Figure 5. (A) Photograph and (B) UV−vis absorption spectra of the AuNPs against different numbers of HL-60 cells: 0, 10, 50, 10^2, 2×10^2, 5×10^2, 1×10^3, 2×10^3, 5×10^3, and 1×10^4 cells. (C) Plot of the absorption ratio (A_{525}/A_{680}) versus different numbers of cancer cells; the inset shows a linear relationship (R^2 = 0.989) with the logarithmic value of cells numbering in the range from 10 to 1×10^4 cells. Error bars represent the standard deviation of three measurements.

line), and the noise ratio did not obviously change (red line). Therefore, 20U NEase and 90 min of nicking time were selected to achieve a good signal-to-noise ratio for the detection of cancer cells.

To investigate the stability of the probe against nuclease, 2 μg of DNase I endonuclease was added into 1 mL of mDNAs-Apt-MBs probe (dispersed in Tris-HCl buffer) in advance and then analyzed with the method proposed, as shown in Figure S3. Whether with or without the target cells (1×10^4 cells), the ratio of two absorbance peaks (A_{525}/A_{680}) shows a negligible difference in the absence (red bars) and presence (black bars) of DNase I endonuclease, indicating the good probe stability of this colorimetric strategy in the presence of DNase I.

Application of the Colorimetric Aptasensor for Detection of HL-60 Cells. To further characterize the sensitivity and the detection range of this assay, a series of samples containing different numbers of target cells have been tested. The photographs of the Au NP colloid, after the addition of target cells ranging from 0 to 1.0×10^4 cells/mL, were plotted in Figure 5A. The color of the Au NP colloid gradually changed from blue to purple and then red with the increasing amount of target cells. In addition to visual analysis, the sensitivity of the assay was further verified by UV−vis spectroscopy (Figure 5B). Along with the increase of the cell concentration, the broad peak (650−750 nm) gradually shifted and disappeared, while the absorbance at 525 nm increased. That is, with the increased number of target cells, the released mDNAs and cleaved ssDNAs increased correspondingly, and the more dispersive (rather than aggregated) Au NPs were present in high salt solution. Accordingly, the absorbance peak ratio of A_{525}/A_{680} was employed to quantitatively scale the cell concentration (Figure 5C). A detection limit of 10 cells for naked eye detection was achieved, indicating the high sensitivity and great signal amplification of this colorimetric aptasensor. In addition, the synthesized Au NPs showed a zeta potential of −30.79 mV (Figure S1). In contrast, the zeta potential of Au NPs decreased to −34.47 mV after adding the suspension resulted from two-round amplification (1.0×10^4 cells/mL), suggesting that cascade colorimetric reaction produced lots of negatively charged ssDNA fragments adsorbed on the surface of Au NPs. In addition, DLS analyses suggested that the hydrodynamic diameter of Au NPs increased due to salt-induced aggregation in the absence of cancer cells. In contrast, when 1×10^4 cells were present, the hydrodynamic diameter was nearly the same as the initially dispersed Au NPs, indicating that salt does not aggregate the Au NPs under this condition due to the enhanced interparticle repulsion (Figure S2).

The as-prepared mDNAs-Apt-MBs probe was used to detect HL-60 cells in diluted FBS. Learned from curve a in Figure S4, the absorbance peak ratio of A_{525}/A_{680} increases with the cancer concentration from 0 to 1×10^4 cells/mL, and the ratio is very close to that of the HL-60 cells detection in buffer solution (b). The results indicate an excellent anti-interference ability of the proposed method in the biological medium.

In order to further investigate the selectivity of the present biosensor for the detection of HL-60 cancer cells, experiments were conducted on PC-12 cancer cells, MCF cancer cells, HeLa cells with the same number (1×10^4 cells), and the blank (no cells). It was also easy to read out from visual observations (Figure 6A). That is, the color of the solution retained red for HL-60 cells while others changed to blue. Figure 6B showed the absorption ratio of A_{525}/A_{680} for the different cells. In the presence of HL-60, the ratio value increased significantly compared with other kinds of cells and the blank. Moreover, the absorbance peak ratio of A_{525}/A_{680} versus different kinds of cancer cells at a series of concentrations was investigated. As shown in Figure S5, the target cells (black) can be distinguished from other kinds of cancer cells whether at a low concentration or a high concentration. Therefore, this colorimetric aptasensor can be applied in the detection of HL-60 cells with high specificity, which was ascribed to a high affinity of the aptamer.

CONCLUSIONS

In this work, we report a novel and intuitive dispersion-dominated colorimetric strategy for highly efficient detection of HL-60 cells based on dual signal amplification, which consists of aptamer scaffold conformational switch and cyclic enzymatic amplification. Instead of modification of Au NPs, ssDNAs produced by dual amplification could be adsorbed on the surface of Au NPs to prevent particle aggregation in high salt environments. This method has significant advantages, such as visualization, simple operation, high sensitivity, and no need for delicate instruments or a sophisticated technologist. In contrast to fluorescence or electrochemical based assays, this colori-

DOI: 10.1021/acsami.5b12117
ACS Appl. Mater. Interfaces 2016, 8, 4434−4441

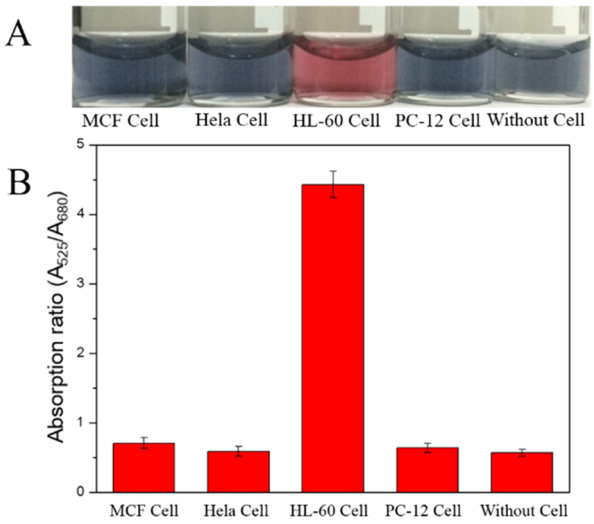

Figure 6. (A) Photograph and (B) the absorption ratio (A_{525}/A_{680}) of the sensing system in the presence of different cells, MCF-7 (1×10^4 cells), Hela (1×10^4 cells), HL-60 (1×10^4 cells), PC-12 (1×10^4 cells), and blank. Error bars represent the standard deviation of three measurements.

metric method could be performed with naked eyes or normal UV−vis spectroscopy. Under optimal conditions, the color change caused by 10 target cells can be distinguished by naked eyes. The approach proposed in this study can be extended to other cancer cells and offers a new approach for developing low cost, sensitive, and rapid cancer cell sensors for potential application in point-of-care cancer diagnosis.

■ ASSOCIATED CONTENT

Supporting Information

The Supporting Information is available free of charge on the ACS Publications website at DOI: 10.1021/acsami.5b12117.

Sequences of the used oligonucleotides, zeta-potential characterization, dynamic light scattering characterization of the size distribution, probe stability affected by DNase 1, serum sample detection, and specific detection of different kinds of cancer cells at various concentrations (PDF)

■ AUTHOR INFORMATION

Corresponding Authors

*Tel./Fax: +86-25-89687294. E-mail: xujj@nju.edu.cn.
*Tel./Fax: +86-25-89684862. E-mail: hychen@nju.edu.cn.

Notes

The authors declare no competing financial interest.

■ ACKNOWLEDGMENTS

This work was supported by the 973 Program (Grant 2012CB932600, 2013CB933802) and the National Natural Science Foundation of China (Grant Nos. 21327902 and 21135003). This work was also supported by the Priority Academic Program Development of Jiangsu Higher Education Institutions.

■ REFERENCES

(1) Uhr, J. W. One-Stop Shop. *Nature* **2007**, *450*, 1168−1169.
(2) Ebert, M. P.; Korc, M.; Malfertheiner, P.; Rocken, C. Advances, Challenges, and Limitations in Serum-Proteome-Based Cancer Diagnosis. *J. Proteome. Res.* **2006**, *5*, 19−25.
(3) Savage, N. Early Detection: Spotting the First Signs. *Nature* **2011**, *471*, S14−S15.
(4) Tan, W.; Donovan, M. J.; Jiang, J. Aptamers from Cell-Based Selection for Bioanalytical Applications. *Chem. Rev.* **2013**, *113*, 2842−2862.
(5) Ellington, A. D.; Szostak, J. W. In Vitro Selection of RNA Molecules that Bind Specific Ligands. *Nature* **1990**, *346*, 818−822.
(6) Yang, C. J.; Jockusch, S.; Vicens, M.; Turro, N. J.; Tan, W. Light-Switching Excimer Probes for Rapid Protein Monitoring in Complex Biological Fluids. *Proc. Natl. Acad. Sci. U. S. A.* **2005**, *102*, 17278−17283.
(7) Tian, C. Y.; Xu, J. J.; Chen, H. Y. A Novel Aptasensor for the Detection of Adenosine in Cancer Cells by Electrochemiluminescence of Nitrogen Doped TiO2 Nanotubes. *Chem. Commun.* **2012**, *48*, 8234−8236.
(8) Chen, C.; Song, G.; Ren, J.; Qu, X. A Simple and Sensitive Colorimetric pH Meter Based on DNA Conformational Switch and Gold Nanoparticle Aggregation. *Chem. Commun.* **2008**, *46*, 6149−6151.
(9) Medley, C. D.; Smith, J. E.; Tang, Z.; Wu, Y.; Bamrungsap, S.; Tan, W. Gold Nanoparticle-Based Colorimetric Assay for the Direct Detection of Cancerous Cells. *Anal. Chem.* **2008**, *80*, 1067−1072.
(10) Wang, K.; Fan, D.; Liu, Y.; Wang, E. Highly Sensitive and Specific Colorimetric Detection of Cancer Cells via Dual-Aptamer Target Binding Strategy. *Biosens. Bioelectron.* **2015**, *73*, 1−6.
(11) Lin, Y. Z.; Chang, P. L. Colorimetric Determination of DNA Methylation Based on the Strength of the Hydrophobic Interactions between DNA and Gold Nanoparticles. *ACS Appl. Mater. Interfaces* **2013**, *5*, 12045−12051.
(12) Shi, H.; He, X.; Wang, K.; Wu, X.; Ye, X.; Guo, Q.; Tan, W.; Qing, Z.; Yang, X.; Zhou, B. Activatable Aptamer Probe for Contrast-Enhanced in Vivo Cancer Imaging Based on Cell Membrane Protein-Triggered Conformation Alteration. *Proc. Natl. Acad. Sci. U. S. A.* **2011**, *108*, 3900−3905.
(13) Song, Y.; Zhu, Z.; An, Y.; Zhang, W.; Zhang, H.; Liu, D.; Yu, C.; Duan, W.; Yang, C. J. Selection of DNA Aptamers against Epithelial Cell Adhesion Molecule for Cancer Cell Imaging and Circulating Tumor Cell Capture. *Anal. Chem.* **2013**, *85*, 4141−4149.
(14) Chandra, P.; Noh, H. B.; Shim, Y. B. Cancer Cell Detection Based on the Interaction between an Anticancer Drug and Cell Membrane Components. *Chem. Commun.* **2013**, *49*, 1900−1902.
(15) Bi, S.; Ji, B.; Zhang, Z.; Zhang, S. A Chemiluminescence Imaging Array for the Detection of Cancer Cells by Dual-Aptamer Recognition and Bio-Bar-Code Nanoprobe-Based Rolling Circle Amplification. *Chem. Commun.* **2013**, *49*, 3452−3454.
(16) Zhu, Y.; Chandra, P.; Shim, Y. B. Ultrasensitive and Selective Electrochemical Diagnosis of Breast Cancer Based on a Hydrazine-Au Nanoparticle-Aptamer Bioconjugate. *Anal. Chem.* **2013**, *85*, 1058−1064.
(17) Liu, J.; Zhou, H.; Xu, J. J.; Chen, H. Y. An Effective DNA-Based Electrochemical Switch for Reagentless Detection of Living Cells. *Chem. Commun.* **2011**, *47*, 4388−4390.
(18) Bamrungsap, S.; Chen, T.; Shukoor, M. I.; Chen, Z.; Sefah, K.; Chen, Y.; Tan, W. H. Pattern Recognition of Cancer Cells Using Aptamer-Conjugated Magnetic Nanoparticles. *ACS Nano* **2012**, *6*, 3974−3981.
(19) Min, H.; Jo, S. M.; Kim, H. S. Efficient Capture and Simple Quantification of Circulating Tumor Cells Using Quantum Dots and Magnetic Beads. *Small* **2015**, *11*, 2536−2542.
(20) Mao, S.; Chang, J.; Zhou, G.; Chen, J. Nanomaterial-Enabled Rapid Detection of Water Contaminants. *Small* **2015**, *11*, 5336−5359.
(21) Zhang, X.; Yin, J.; Yoon, J. Recent Advances in Development of Chiral Fluorescent and Colorimetric Sensors. *Chem. Rev.* **2014**, *114*, 4918−4959.
(22) Sun, H.; Zu, Y. Aptamers and Their Applications in Nanomedicine. *Small* **2015**, *11*, 2352−2364.

DOI: 10.1021/acsami.5b12117
ACS Appl. Mater. Interfaces 2016, 8, 4434−4441

(23) Lu, C.; Liu, X.; Li, Y.; Yu, F.; Tang, L.; Hu, Y.; Ying, Y. Multifunctional Janus Hematite-Silica Nanoparticles: Mimicking Peroxidase-Like Activity and Sensitive Colorimetric Detection of Glucose. *ACS Appl. Mater. Interfaces* **2015**, *7*, 15395−15402.
(24) Song, Y.; Wei, W.; Qu, X. Colorimetric Biosensing Using Smart Materials. *Adv. Mater.* **2011**, *23*, 4215−4236.
(25) Feng, J. J.; Guo, H.; Li, Y. F.; Wang, Y. H.; Chen, W. Y.; Wang, A. J. Single Molecular Functionalized Gold Nanoparticles for Hydrogen-Bonding Recognition and Colorimetric Detection of Dopamine with High Sensitivity and Selectivity. *ACS Appl. Mater. Interfaces* **2013**, *5*, 1226−1231.
(26) Xiao, Q.; Gao, H.; Lu, C.; Yuan, Q. Gold Nanoparticle-Based Optical Probes for Sensing Aminothiols. *TrAC, Trends Anal. Chem.* **2012**, *40*, 64−76.
(27) Li, K.; Qin, W.; Li, F.; Zhao, X.; Jiang, B.; Wang, K.; Deng, S.; Fan, C.; Li, D. Nanoplasmonic Imaging of Latent Fingerprints and Identification of Cocaine. *Angew. Chem., Int. Ed.* **2013**, *52*, 11542−11545.
(28) Wang, J.; Wang, L.; Liu, X.; Liang, Z.; Song, S.; Li, W.; Li, G.; Fan, C. A Gold Nanoparticle-Based Aptamer Target Binding Readout for ATP Assay. *Adv. Mater.* **2007**, *19*, 3943−3946.
(29) Zhang, Z.; Chen, Z.; Wang, S.; Qu, C.; Chen, L. On-Site Visual Detection of Hydrogen Sulfide in Air Based on Enhancing the Stability of Gold Nanoparticles. *ACS Appl. Mater. Interfaces* **2014**, *6*, 6300−6307.
(30) Lu, W. T.; Arumugam, R.; Senapati, D.; Singh, A. K.; Arbneshi, T.; Khan, S. A.; Yu, H. T.; Ray, P. C. Multifunctional Oval-Shaped Gold-Nanoparticle-Based Selective Detection of Breast Cancer Cells Using Simple Colorimetric and Highly Sensitive Two-Photon Scattering Assay. *ACS Nano* **2010**, *4*, 1739−1749.
(31) Ye, X.; Shi, H.; He, X.; Wang, K.; He, D.; Yan, L.; Xu, F.; Lei, Y.; Tang, J.; Yu, Y. Iodide-Responsive Cu-Au Nanoparticle-Based Colorimetric Platform for Ultrasensitive Detection of Target Cancer Cells. *Anal. Chem.* **2015**, *87*, 7141−7147.
(32) Chen, S.; Chu, L. T.; Yeung, P. P.; Zhao, Z.; Bao, Y.; Chan, M. S.; Lo, P. K.; Chen, T. H. Enzyme-Free Amplification by Nano Sticky Balls for Visual Detection of ssDNA/RNA Oligonucleotides. *ACS Appl. Mater. Interfaces* **2015**, *7*, 22821−22830.
(33) Li, J.; Fu, H. E.; Wu, L. J.; Zheng, A. X.; Chen, G. N.; Yang, H. H. General Colorimetric Detection of Proteins and Small Molecules Based on Cyclic Enzymatic Signal Amplification and Hairpin Aptamer Probe. *Anal. Chem.* **2012**, *84*, 5309−5315.
(34) Zhang, X.; Xiao, K.; Cheng, L.; Chen, H.; Liu, B.; Zhang, S.; Kong, J. Visual and Highly Sensitive Detection of Cancer Cells by a Colorimetric Aptasensor Based on Cell-Triggered Cyclic Enzymatic Signal Amplification. *Anal. Chem.* **2014**, *86*, 5567−5572.
(35) Yin, B. C.; Liu, Y. Q.; Ye, B. C. One-Step, Multiplexed Fluorescence Detection of microRNAs Based on Duplex-Specific Nuclease Signal Amplification. *J. Am. Chem. Soc.* **2012**, *134*, 5064−5067.
(36) Connolly, A. R.; Trau, M. Isothermal Detection of DNA by Beacon-Assisted Detection Amplification. *Angew. Chem., Int. Ed.* **2010**, *49*, 2720−2723.
(37) Zhang, J.; Wang, L.; Pan, D.; Song, S.; Boey, F. Y.; Zhang, H.; Fan, C. Visual Cocaine Detection with Gold Nanoparticles and Rationally Engineered Aptamer Structures. *Small* **2008**, *4*, 1196−1200.
(38) Li, H.; Rothberg, L. Colorimetric Detection of DNA Sequences Based on Electrostatic Interactions with Unmodified Gold Nanoparticles. *Proc. Natl. Acad. Sci. U. S. A.* **2004**, *101*, 14036−14039.
(39) Sun, W.; Lu, Y.; Mao, J.; Chang, N.; Yang, J.; Liu, Y. Multidimensional Sensor for Pattern Recognition of Proteins Based on DNA-Gold Nanoparticles Conjugates. *Anal. Chem.* **2015**, *87*, 3354−3359.
(40) Li, H.; Rothberg, L. J. Label-Free Colorimetric Detection of Specific Sequences in Genomic DNA Amplified by the Polymerase Chain Reaction. *J. Am. Chem. Soc.* **2004**, *126*, 10958−10961.
(41) Liu, J.; Lu, Y. Preparation of Aptamer-Linked Gold Nanoparticle Purple Aggregates for Colorimetric Sensing of Analytes. *Nat. Protoc.* **2006**, *1*, 246−252.
(42) Li, C.; Lin, J.; Guo, Y.; Zhang, S. A Novel Electrochemiluminescent Reagent of Cyclometalated Iridium Complex-Based DNA Biosensor and Its Application in Cancer Cell Detection. *Chem. Commun.* **2011**, *47*, 4442−4444.
(43) Li, J. J.; Chu, Y.; Lee, B. Y.; Xie, X. S. Enzymatic Signal Amplification of Molecular Beacons for Sensitive DNA Detection. *Nucleic Acids Res.* **2008**, *36*, e36.
(44) Xue, L.; Zhou, X.; Xing, D. Sensitive and Homogeneous Protein Detection Based on Target-Triggered Aptamer Hairpin Switch and Nicking Enzyme Assisted Fluorescence Signal Amplification. *Anal. Chem.* **2012**, *84*, 3507−3513.
(45) Yang, B.; Zhang, X. B.; Kang, L. P.; Shen, G. L.; Yu, R. Q.; Tan, W. Target-Triggered Cyclic Assembly of DNA-Protein Hybrid Nanowires for Dual-Amplified Fluorescence Anisotropy Assay of Small Molecules. *Anal. Chem.* **2013**, *85*, 11518−11523.

DOI: 10.1021/acsami.5b12117
ACS Appl. Mater. Interfaces 2016, 8, 4434−4441